Appearance of the second dip in elastic pp scattering

D. J. Clarke and S. Y. Lo
School of Physics, University of Melbourne, Parkville, Victoria 3052, Australia
(Received 17 April 1978)

One form of a Chou-Yang model is used successfully to fit all pp data for $P_{\text{Lab}} = 50$ to 1500 GeV/c, and $-t = 0.0$ to 12 GeV^2 with a differential cross section that runs twelve orders of magnitude from 10^2 mb/GeV^2 to 10^{-10} mb/GeV^2. The t dependence is fixed by the proton form factors alone, and there is only one free energy-dependent parameter $\mu_1(s)$ in the model. Specific predictions concerning the appearance of a second minimum in the pp differential cross section are made.

I. INTRODUCTION

Since the initial experimental verification of the existence of a minimum in the pp differential cross section,[1] further experiments have confirmed the predictions made at that time,[2] using the current-current interaction reformulation of the Chou-Yang model.[3] In addition to providing excellent fits to the then available experimental data, the model anticipated the observed[4] change in position of the diffraction minimum with energy and the increase with energy of the second peak. Since that time data[5-8] have become available covering a broad range of energies and, more recently, extending to large $|t|$. Discussion has arisen concerning the non-appearance of the predicted second minimum.[9] This paper has a twofold purpose: firstly, to demonstrate the ability of the current-current interaction form of the Chou-Yang model to accommodate all new data and, secondly, to make some specific predictions concerning the development of the second dip.

The agreement with data is excellent for a range of values that runs through twelve orders of magnitude in $d\sigma/dt$ from 10^2 mb/GeV^2 at $t \simeq 0$ to 10^{-10} mb/GeV^2 at $t \sim 12$ GeV^2. The magnitude of the coupling for the vacuum exchange part is determined by $\sigma_{\text{tot}}(pp)$ from the optical theorem, and the only free parameter is the energy-dependent parameter $\mu_1(s)$. The t dependence of the model is completely determined by the proton form factors. From such a good fit we argue that the non-appearance of the second dip at $P_{\text{lab}} = 1500$ GeV/c is not at all surprising, and that it probably will reveal itself in the next generation of accelerator energy.

II. DISCUSSION OF THE CURRENT-CURRENT FORM OF THE CHOU-YANG MODEL

In the eikonal approximation, the cross section is

$$\frac{d\sigma}{dt} = |\alpha(t)|^2 \tag{2.1}$$

and the scattering amplitude is given by

$$\alpha(\vec{K}^2) = \int \frac{d^2b}{2\pi}[1 - S(b)]e^{i\vec{K}\cdot\vec{b}}, \tag{2.2}$$

where $\vec{K}$ and $\vec{b}$ are two-dimensional vectors, $\vec{b}$ is the impact parameter, and $\vec{K}^2$ is the momentum transfer squared. The Chou-Yang model makes a very specific assumption as to the form of $S(b)$ for nucleon-nucleon (NN) scattering,

$$S(\vec{b}) = \exp\left[-\sum_j \int\int \rho_N^j(x)\rho_N^j(x') \times I^j(\vec{b} - \vec{x}' + \vec{x})d^3x'd^3\vec{x}\right], \tag{2.3}$$

where the summation is over the nucleon density functions with various SU_3 quantum numbers indicated by j. The $j=0$ term is the vacuum-exchange term and the interaction I^0 is taken to be the contact interaction

$$I^0 = \mu_0'\delta^2(\vec{b} - \vec{x}' + \vec{x}). \tag{2.4}$$

However, the interaction where the quantum number is exchanged must be energy dependent:

$$I^j = \mu_j'(s)\delta^2(\vec{b} - \vec{x}' + \vec{x}), \quad j = 3 \text{ or } 8. \tag{2.5}$$

The density functions ρ_N^j are the hadron matter distribution functions of the nucleon. They are related to the nucleon form factor $F^j(K^2)$ by the Fourier transform

$$F^j(q^2) = \frac{1}{2\pi}\int d^3x\, \rho_N^j(x)e^{i\vec{q}\cdot\vec{x}}, \tag{2.6}$$

where $\vec{q} = (K_x, K_y, 0)$.

Quantization is possible through substitution of $\rho(x)$ by quantized field operators

$$\rho(x) \to \psi^\dagger(x)\psi(x). \tag{2.7}$$

It is our interpretation of the Chou-Yang model

that the field operators $\psi^\dagger(x)\psi(x)$ are the fourth component of the current

$$\rho^j(x) \to J_4^j(x). \tag{2.8}$$

Equation (2.3) has now become

$$S(s,\vec{b}) = \exp\Big[-2\pi\mu_0(s) \int\int d^3x\, d^3x' J_4^0(\vec{x},0) J_4^0(\vec{x}',0)\delta^2(\vec{b}-\vec{x}'+\vec{x}) - 2\pi\mu_1(s) \int\int d^3x\, d^3x' J_4^3(\vec{x},0) J_4^3(\vec{x}',0)\delta^2(\vec{b}-\vec{x}'+\vec{x})\Big], \tag{2.9}$$

where J_4^0 and J_4^3 are the fourth components of the isoscalar and isovector currents of the proton and $\mu_j = \mu_j'/2\pi$.

The scattering amplitude $\alpha(s,K^2)$ for the elastic proton-proton scattering is defined by the relation

$$i2\pi^6\delta^2(\vec{k}'-\vec{k}+\vec{K})\delta^2(\vec{p}'-\vec{p}-\vec{K})\delta(k_3'-k_3)\delta(p_3'-p_3)\alpha(s,K^2) = \left\langle p',k' \middle| \int \frac{d^2\vec{b}}{2\pi} \exp(i\vec{K}\cdot\vec{b})[S(s,\vec{b})-1] \middle| p,k \right\rangle, \tag{2.10}$$

where p,k and p',k' are the incoming and outgoing four-momenta of the protons, and $\vec{K}^2 = -t$ is the transverse momentum squared.

The amplitude may be decomposed into a sum of two terms, $\alpha_0(s,K^2)$, the vacuum-exchange term, and $\alpha_1(s,K^2)$, the $I=1$ exchange term:

$$-i\alpha_0(s,K^2) = \mu_0(s)\langle\vec{K}|J_4^0(0)|0\rangle\langle-\vec{K}|J_4^0(0)|0\rangle - \frac{\mu_0^2(s)}{2!}\int\frac{d^2K'}{2\pi}\sum_{\text{spin}}\langle\vec{K}|J_4^0(0)|\vec{K}'\rangle\langle\vec{K}'|J_4^0(0)|0\rangle\langle-\vec{K}|J_4^0(0)|-\vec{K}'\rangle\langle-\vec{K}'|J_4^0(0)|0\rangle + \cdots, \tag{2.11}$$

$$-i\alpha_1(s,K^2) = \mu_1(s)\langle\vec{K}|J_4^3(0)|0\rangle\langle-\vec{K}|J_4^3(0)|0\rangle \tag{2.12}$$

The matrix element of a unitary current between proton states can be written

$$\langle p'|J_4^0(0)|p\rangle = \left(\frac{m^2}{p_0 p_0'}\right)^{1/2}\bar{u}(p')\Big[F_1^j(q^2)\gamma_4 + F_2^j(q^2)\frac{1}{2m}\sigma_{i4}q_i\Big]u(p). \tag{2.13}$$

Omission of the spin-flip term F_2^j, in the infinite momenta frame leads to

$$\langle\vec{K}|J_4^0(0)|0\rangle = F_p^0(\vec{K}^2), \tag{2.14}$$

and the alternating signs in Eq. (2.11) produce the zeros which characterize the Chou-Yang model. However, since we have the additional term F_2^j contributing to the spin-flip amplitudes, we do not have any zeros in (2.11), even in the asymptotic limit.

The isovector form factors which enter into the calculation of $\alpha_1(s,\vec{K}^2)$ are well known and we again[3] take the singlet form factors of $\alpha_0(s,\vec{K}^2)$ to be the familiar isoscalar form factors, and use the convenient dipole formulas.

For numerical calculation we use a sum of four Gaussians to simulate the dipole formula. The val-

TABLE I. The parametric form of the form factors $F_A(K^2)F_B(K^2)=\sum_i a_i e^{-b_i K^2}$.

Form factors	a_1	b_1 (GeV^{-2})	a_2	b_2 (GeV^{-2})	a_3	b_3 (GeV^{-2})	a_4	b_4 (GeV^{-2})
(1) Isoscalar $F_{1S}{}^2(K^2)$	7.141×10^{-1}	6.954×10^{0}	1.009×10^{-2}	7.815×10^{-1}	1.63×10^{-4}	2.429×10^{-1}	2.756×10^{-1}	2.394×10^{0}
(2) Isovector $F_{1V}{}^2(K^2)$	5.499×10^{-1}	4.729×10^{0}	3.915×10^{-1}	1.800×10^{0}	5.483×10^{-2}	6.913×10^{-1}	2.100×10^{-3}	2.295×10^{-1}
(3) Isoscalar products $-F_{1S}F_{2S}$	5.763×10^{-2}	8.288×10^{0}	4.639×10^{-2}	3.421×10^{0}	1.236×10^{-2}	4.969×10^{0}	3.618×10^{-3}	1.228×10^{0}

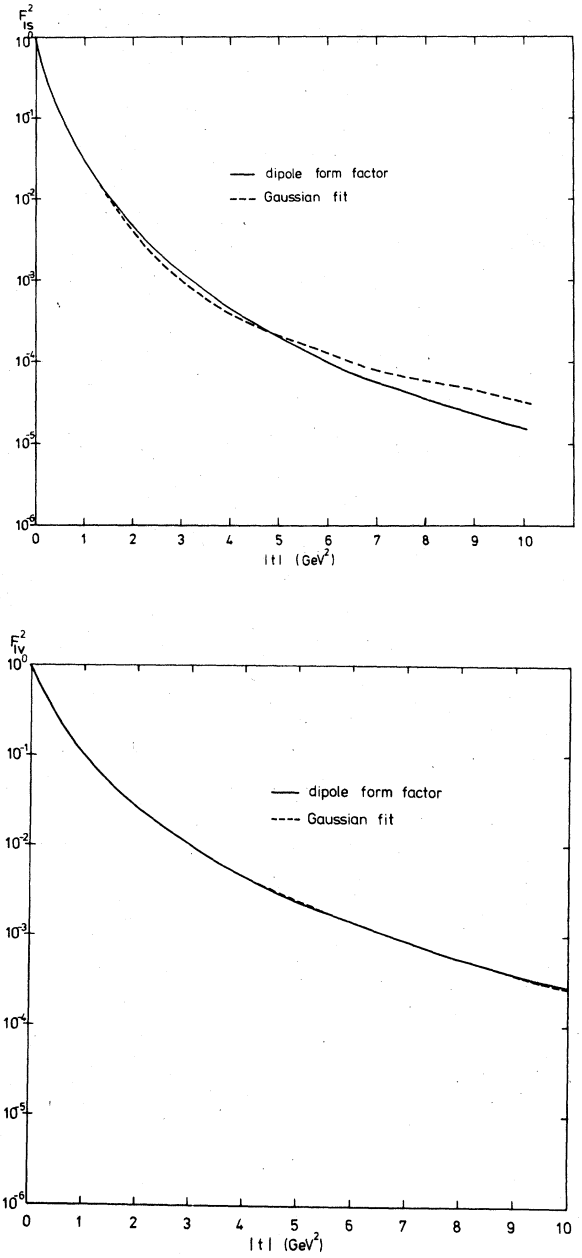

FIG. 1. Gaussian fits to the dipole formula for the various form-factor combinations. The solid curves represent $F_{1S}{}^2$ and $F_{1V}{}^2$ respectively, calculated using the dipole formula. The broken curves represent the sum of four Gaussians used in numerical calculations to simulate the form-factor combinations.

ues we use are listed in Table I, and the Gaussian fits to the dipole formula are shown in Fig. 1. We calculate to the ninth order in the vacuum-exchange spin-nonflip term, second order in spin-flip vacuum exchange term, and only first order in the energy-dependent $I=1$ exchange term.

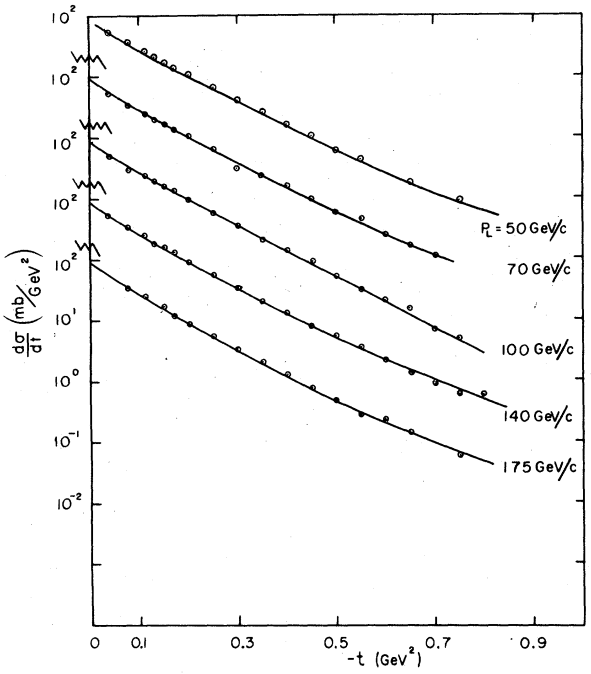

FIG. 2. Theoretical fits to pp elastic scattering differential-cross-section data (Ref. 8) over the total-cross-section range 38.2 to 39.0 mb (P_{lab}=50, 70, 100, 140, 175 GeV/c), for $-t \leq 0.8$ GeV^2. A specific energy dependence $\mu_1(s) = (20/s^{2/3})e^{i\phi}$ provides a good fit to these data.

Since the total cross section for pp scattering is

$$\sigma_{tot} = 4\pi(\alpha_0 + \mathrm{Im}\alpha_1) \tag{2.15}$$

σ_{tot} serves as input for numerical calculations to fix $u_0(s)$ which has the parametric form

$$\mu_0(s) = \mu + \mu' \left| \ln\left(\frac{s}{s_0}\right) \right|^2 \tag{2.16}$$

with $\mu = 9.76$ GeV^{-2}, $\mu' = 0.23$ GeV^{-2}, and $s_0 = 200$ GeV^2.

No simple energy dependence has yet been found for $\mu_1(s)$ which at present must be determined empirically (for each cross section) at each energy Further data covering a broad energy range and extending to large $|t|$ are needed if the structure of $\mu_1(s)$ is to reveal itself. Excellent fits were produced to data[8] at small t ($|t| \leq 0.8$ GeV^2) for equivalent laboratory momenta of 50, 70, 100, 140, and 175 GeV/c, using

$$\mu_1(s) = \frac{20}{s^{2/3}} e^{i\phi},$$

where ϕ is the phase angle.

This is shown in Fig. 2. However, data at higher energies and large $|t|$ indicate an energy dependence becoming increasingly gradual,[12] although

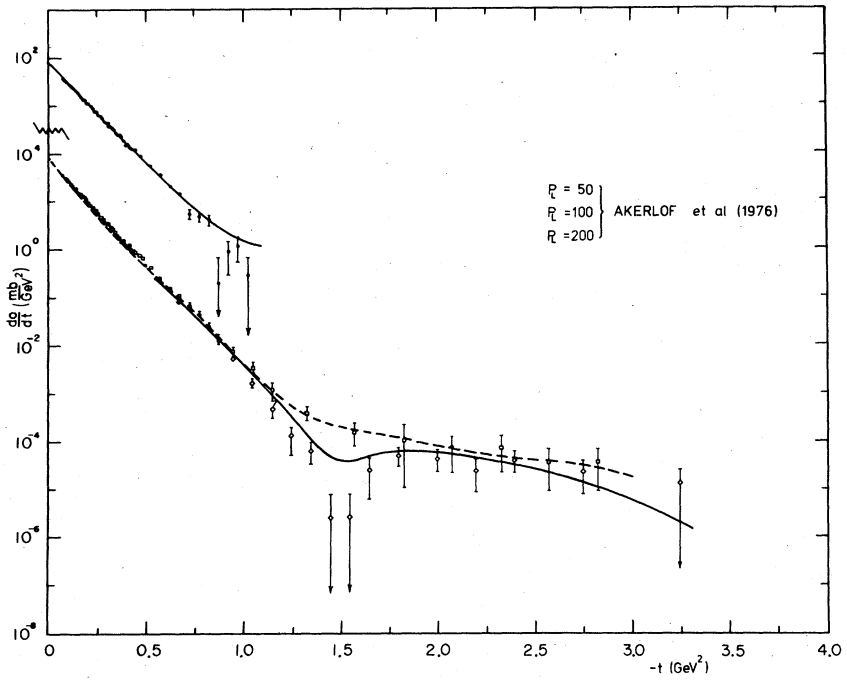

FIG. 3. Theoretical fits to pp elastic scattering data (Ref. 5) corresponding to total cross sections of 38.97 ± 0.04 mb (P_{lab}=200 GeV/c), 38.46 ± 0.04 mb (P_{lab}=100 GeV/c), and 38.20 ± 0.05 mb (P_{lab}=50 GeV/c) for $0 \leq -t < 3.4$ GeV^2. [Total cross sections used are from A. S. Carroll *et al.*, Phys. Lett. 61B, 303 (1976).] The broken line is the curve for P_{lab}=100 GeV/c, and the values of μ_1 used are 0.80, 0.22, and 0.11 for P_{lab}=50, 100, and 200 GeV/c respectively.

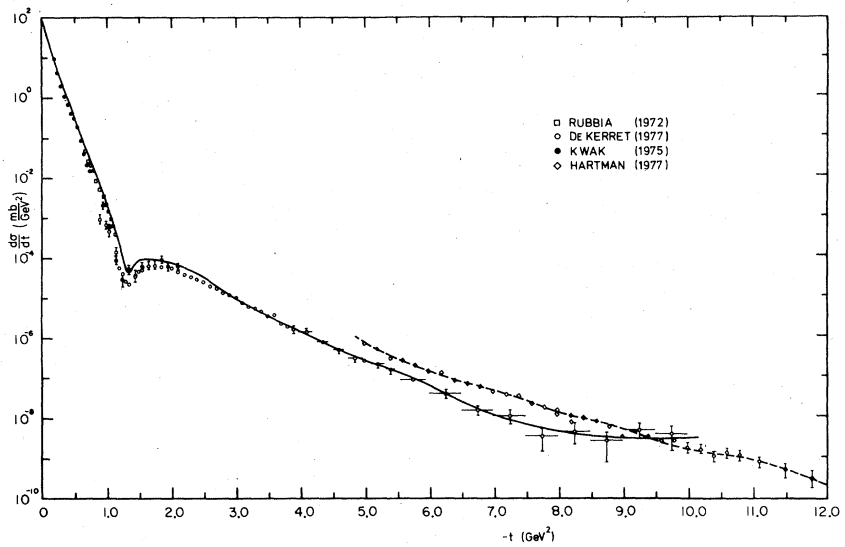

FIG. 4. Theoretical fits to ISR data (Refs. 1, 4, and 7) and large-$|t|$ data for $\sigma_{tot}=39$ mb ($P_{lab}=200$ GeV/c) (Ref. 6). Total cross sections corresponding to ISR data are 42.5 ± 0.27 mb (Rubbia and De Kerret, $P_{lab}=1480$ GeV/c and 1500 GeV/c respectively) and 43.04 ± 0.31 mb (Kwak, $P_{lab}=2052$ GeV/c). The theoretical curve used to fit the ISR data has an input total cross section of 42.8 mb and $\mu_1=0.100$. The broken line is the curve for $P_{lab}=200$ GeV/c with $\mu_1=0.110$.

still at least $s^{-1/2}$ at present CERN ISR energies.[6] The phase ϕ is found to vary with the square of the four-momentum transfer $-t=K^2$.

All theoretical curves for the differential cross section are therefore given with both their corresponding total cross section and the numerical value of μ_1. These two parameters determine the energy dependence of the model.

In Fig. 3 theoretical curves are drawn for the differential cross section at laboratory momenta of 50, 100, and 200 GeV/c. These fits are quite good. The greatest error for $P_{lab}=50$ GeV/c is 14% at $-t=0.30$ GeV, and the greatest error at 100 GeV/c is 35% at $-t=0.45$ GeV^2. For $P_{lab}=200$ GeV/c the area of greatest discrepancy is in the dip region, with the theoretical cross section agreeing well with experiment for all the remaining $|t|$ range.

It is in the proximity of the dips that the $I=1$ exchange term and the spin-flip amplitudes as-

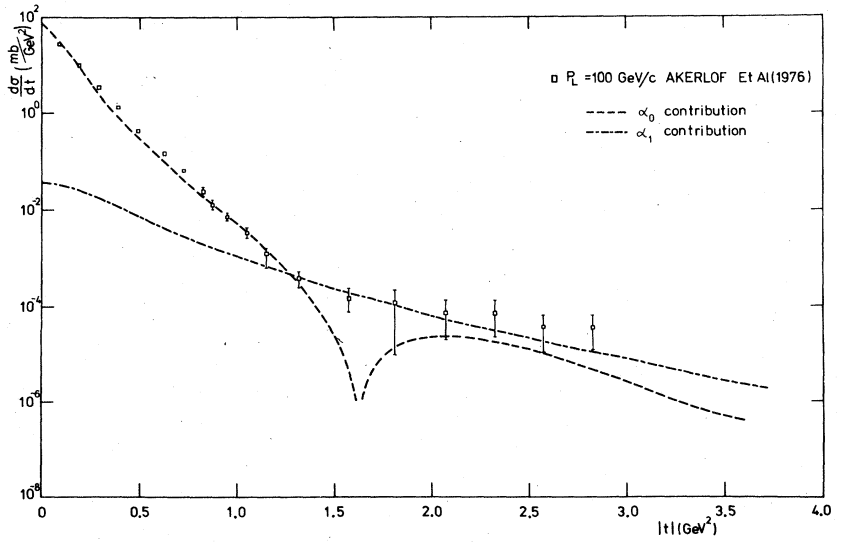

FIG. 5. The relative magnitudes of the α_0 and α_1 contributions to $d\sigma/dt$ at $P_{lab}=100$ GeV/c. (Data are from Ref. 5).

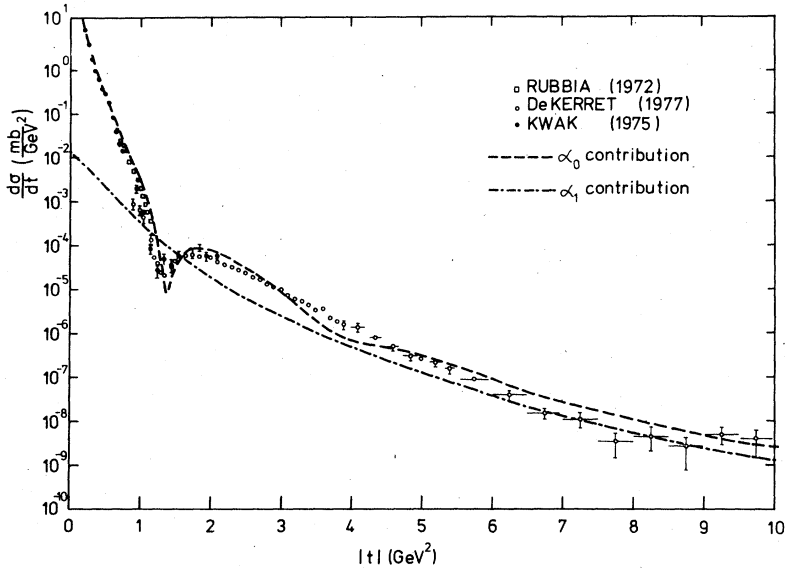

FIG. 6. The relative magnitudes of the α_0 and α_1 contributions to $d\sigma/dt$ at $P_{lab}=1500$ GeV/c (ISR energies). Data are taken from Refs. 1, 4, and 7.

sume the greatest relative importance. Greater accuracy will be possible once the spin-flip amplitudes are included to sufficiently high order in the numerical calculations. At present, Eq. (2.11) is being computed to ninth order in spin-nonflip terms involving only F_1^0, but only to second order in spin-flip terms with F_2^0. The smaller energy-dependent amplitude $\alpha_1(s, \vec{K}^2)$ is included to first order.

Figure 4 provides excellent fits to available high-$|t|$ data. The theoretical curve for $P_{lab}=1500$ GeV/c uses an input total cross section of 42.8 mb and $\mu_1=0.100$ GeV^{-2} to obtain a very good fit over the range $0 \leq -t \leq 10$ GeV^2. The fit to $P_{lab}=200$ GeV/c is similarly good.

Figures 5 and 6 show the relative magnitudes of the α_0 and α_1 contributions to the cross section at 100 GeV/c and 1500 GeV/c respectively. This

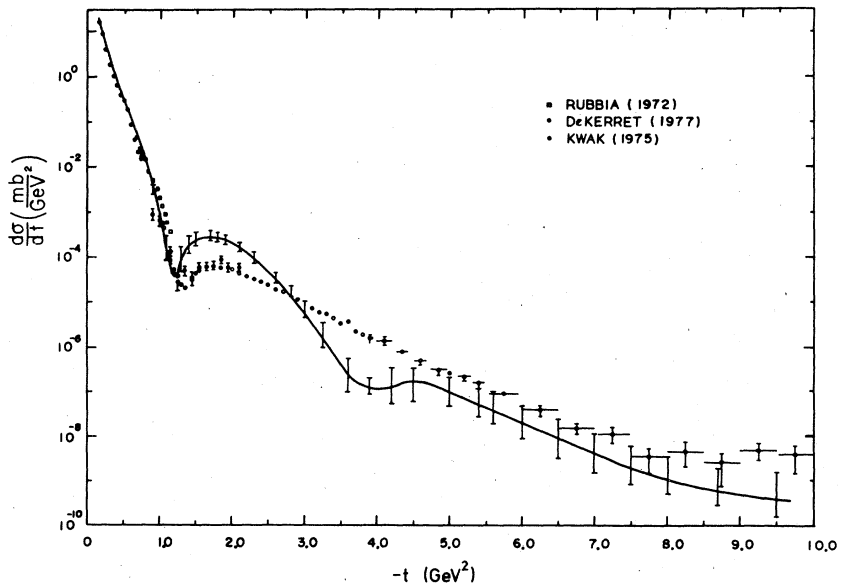

FIG. 7. Theoretical curve for $\sigma_{tot}=49.1$ mb ($P_{lab}=6000$ GeV/c) using $\mu_1=0.050$. The "error" bars superimposed on the curve indicate the range of $d\sigma/dt$ values accessible at given $|t|$ through variation of the phase. The spin-flip contribution has been suppressed. (Data are at ISR energies from Refs. 1, 4, and 7).

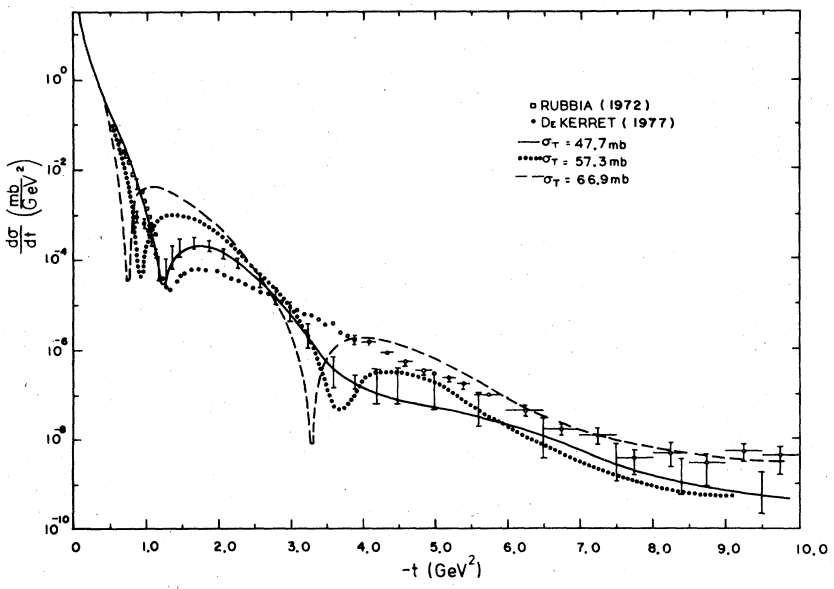

FIG. 8. Theoretical curves for $\sigma_{tot}=47.7$ mb ($P_{lab}=4500$ GeV/c), $\sigma_{tot}=57.3$ mb ($P_{lab}=24\,000$ GeV/c), and $\sigma_{tot}=66.9$ mb ($P_{lab}=104\,167$ GeV/c) $\mu_1=0.0577$, 0.025, and 0.012 respectively. The spin-flip contribution has been suppressed. Theoretical "error" bars apply to the $P_{lab}=4500$-GeV/c curve and indicate the range accessible through phase variation.

does not include the cross-product term which incorporates the phase. For the significance of this term refer to the "error bars" of Figs. 7 and 8.

The range of values fit for the $d\sigma/dt$ covers twelve orders of magnitude from 10^2 mb/GeV^2 in the forward direction to 10^{-10} at $-t=12.0$ GeV^2. One should notice that the first dip is filled in below $P_{lab}=200$ GeV/c, and one would not notice there is a diffractive zero if one's accelerator energy has not exceeded 200 GeV/c. Similarly, we argue that there is not yet a dip at $|t|=3$GeV^2 because the present energy is still not high enough. In the next section we shall discuss more fully when the second dip is most likely to be seen.

III. THE APPEARANCE OF THE SECOND MINIMUM

The zeros of the original Chou-Yang model[10] are well known. In our particular version of the Chou-Yang model, where the current-current interaction form is used, these zeros are filled in with spin-flip amplitudes leading to the appearance of minima but not zeros in the asymptotic energy. The full details will be discussed separately in a different paper.[11] In general, the qualitative features of the Chou-Yang model stay the same for different versions of form factors used.

At finite energy there is, in addition, an amplitude due to $I=1$ exchange, which will fill in the dip. This effect overwhelms the spin-flip amplitude of the vacuum exchange term. For the present section, we shall suppress the spin-flip amplitude and discuss only the effect of the energy-dependent $I=1$ exchange term, which controls the filling up of the first and second dip.

With regard to the $I=1$ exchange term, it is uncertain at present the form taken by the energy-dependent interaction $\mu_1(s)$, and the values used are chosen by applying an energy dependence of $s^{-1/2}$ to the value of μ_1 used to fit ISR data. Although it appears[6] that the s dependence of $d\sigma/dt$ is at least $s^{-1/2}$, the energy dependence does appear to become increasingly gradual up to ISR energies so any predictions arising from use of $s^{-1/2}$ must be interpreted as a lower limit on the energy at which the dip might appear. A further uncertainty exists as to the choice of phase of μ_1. Our model cannot prescribe the phase.

The theoretical curves shown in Figs. 7 and 8 are examples of the many curves which could be drawn within the range possible through phase variation. It is clear, even allowing the range of permitted values at given $|t|$, that for an input total cross section of 47.7 mb ($P_{lab}=4500$ GeV/c), and with $\mu_1=0.0577$, some break in the slope may be expected, and for $\sigma_{tot}=49.1$ mb ($P_{lab}=6000$ GeV/c) and $\mu_1=0.050$ the development of a second minimum should be quite clear.

A further quite sensitive indicator of dip development is the slope parameter $b(s,t)$. In Figs. 9(a) and 9(b) the theoretical slope parameter is plotted for fixed phase, first at present ISR ener-

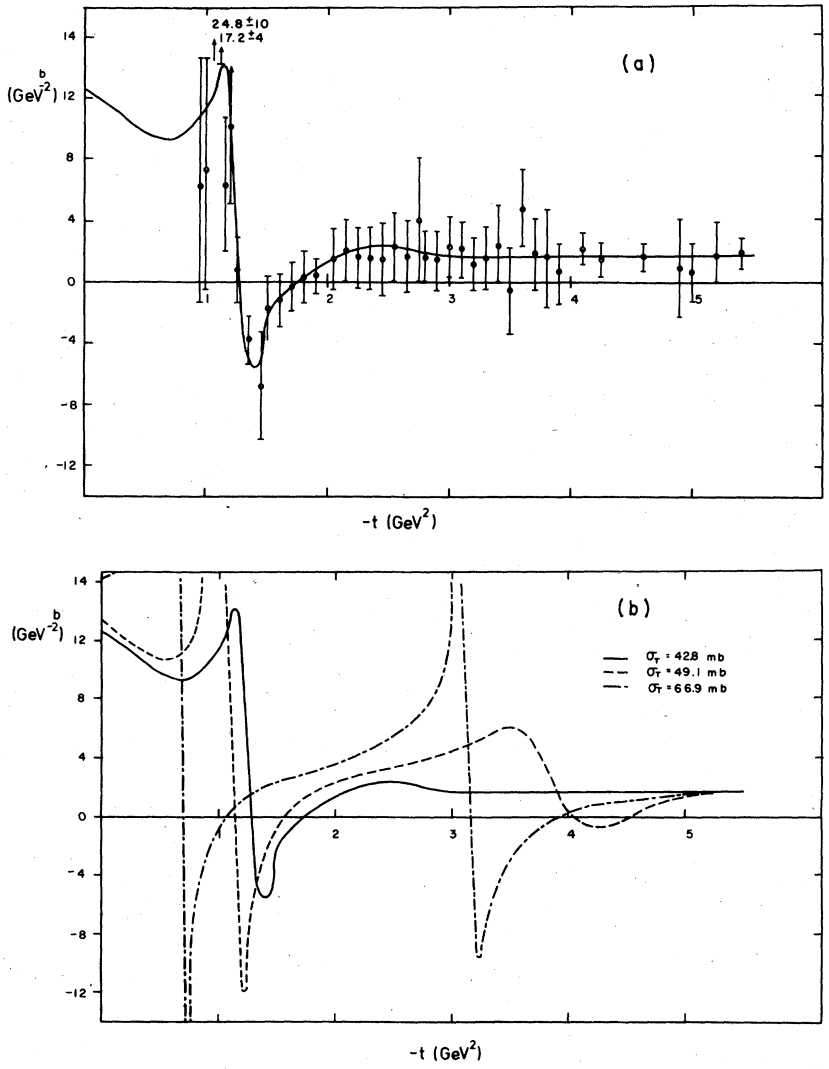

FIG. 9. (a) Slope parameters $b(s,t)$ as a function of momentum transfer squared. Data are calculated from Ref. 7. The solid line is the theoretical curve from the model. (b) Theoretical curves for slope parameter $b(s,t)$ as a function of energy. Solid curve is the fit to ISR data with σ_T=42.8 mb as normalization point. Broken curves correspond to total cross sections of 49.1 mb (P_L=6000 GeV/c) and 66.9 mb (P_L=104 167 GeV/c). For these last two curves the phase is fixed for all $|t|$ in such a way that the value of $d\sigma/dt$ in the region of the second dip is minimized. This would correspond to the slope parameter at the lower end of the theoretical error bars in Fig. 4. Dip appearance is indicated by a change in the sign of the slope parameter.

gies, and then at successively higher energies and correspondingly lower values of μ_1. The development of a minimum is indicated by a change in the sign of the slope parameter.

The energies we discuss here are all within the reach of the next generation of proton accelerators. One interesting point is that the differential cross section around the second dip will still be of the same order as the present ISR values (see Fig. 5). Therefore, the order of magnitude is such that there will be no additional difficulty for the experimentalist to measure.

IV. CONCLUSION

We have successfully demonstrated that the Chou-Yang model with current-current interaction is capable of explaining all the features in the high-energy pp elastic scattering, both qualitatively and quantitatively.

The essential feature of the Chou-Yang model which relates the t dependence of the $d\sigma/dt$ with the proton form factors remains valid. The specific form we use identifies the vacuum-exchange term with the isoscalar nucleon form factors. The

variation of the cross section with energy cannot be predicted within the scheme of the Chou-Yang model and has to be parametrized. This makes the prediction of the exact energy for appearance of the second dip difficult. Nevertheless, if we assume the energy-dependent term to decrease as $1\sqrt{s}$, the second dip should certainly be seen P_{lab} $\sim 10^4$ GeV/c, a quite accessible energy in the next few years.

ACKNOWLEDGMENT

One of the authors (D.J.C.) wishes to thank J. P. Clarke for invaluable assistance.

[1]C. Rubbia, in *Proceedings of the XVI International Conference on High Energy Physics, Chicago-Batavia, Illinois, 1972*, edited by J. D. Jackson and A. Roberts (NAL, Batavia, Ill., 1973), Vol. 4, p. 157.

[2]D. J. Clarke and S. Y. Lo, Phys. Rev. D 10, 1519 (1974).

[3]S. Y. Lo, Nucl. Phys. B 19, 286 (1970).

[4]N. Kwak, *et al.*, Phys. Lett. 58B, 233 (1975).

[5]C. W. Akerlof *et al.*, Phys. Rev. D 14, 2864 (1976).

[6]J. L. Hartmann *et al.*, Phys. Rev. Lett. 39, 975 (1977).

[7]H. De Kerret *et al.*, Phys. Lett. 68B, 374 (1977).

[8]Fermilab Single Arm Spectrometer Group, Phys. Rev. Lett. 35, 1195 (1975).

[9]U. P. Sukatme, Phys. Rev. Lett. 38, 124 (1977).

[10]T. T. Chou and C. N. Yang, Phys. Rev. 170, 1591 (1968); Phys. Rev. Lett. 20, 1213 (1968); Stony Brook Report No. ITP SB 77-67 (unpublished).

[11]D. J. Clarke and S. Y. Lo (unpublished).

[12]This increasingly gradual energy dependence is clearly suggested in H. R. Barton *et al.*, Phys. Rev. Lett. 37, 1659 (1976).